ELSEVIER

Catalysis Today 49 (1999) 23–31

CATALYSIS TODAY

Fluidised bed reactor studies of H_2S decomposition over supported bimetallic Ru catalysts

D. Cao, A.A. Adesina*

Reactor Engineering and Technology Group, School of Chemical Engineering and Industrial Chemistry, University of New South Wales, Sydney, NSW 2052, Australia

Abstract

H_2S is produced in large quantities in the coal, petroleum and mineral processing industries. The decomposition of H_2S to recover both salable sulphur and H_2 which may be recycled for further re-use in upstream hydrodesulphurisation (HDS) units is important in the context of zero-pollutant discharge. Several transition bimetallic sulphide catalysts (with Ru as a constant ingredient) were evaluated in a fluidised bed reactor operated at 160 kPa and 883–1003 K. The Ru–Mo pair emerged as the ''best'' catalyst for H_2 production. The activity of the catalysts was well correlated with the same electronic and metal sulphur bond properties, A-character, seen for HDS reactions. The Ru–Mo catalyst exhibited a first order kinetics in H_2S partial pressure with an activation energy of 69.7 kJ mol^{-1}. Due to thermodynamic limitations H_2 yields are low. This study shows that H_2S conversions in a fluidised bed reactor may be higher than those obtained from a fixed bed configuration operating under same flow conditions. Indeed, conversions in the fluidised bed reactor were higher than equilibrium values near minimum bubbling conditions at all the temperatures examined. However, as the flow rate increased beyond this point, conversion dropped significantly probably due to the onset of slugging. This improved conversion was attributed to the ''membranous effect'' in the fluidised bed since reaction occurs primarily in the emulsion phase and the migration rate of the relatively low molecular weight H_2 product from the catalyst-containing emulsion phase to the solid-free bubble phase helped to shift the reversible reaction in favour of hydrogen.

Keywords: H_2S decomposition; Fluidised bed reactor; Bimetallic catalysts; Ruthenium

1. Introduction

Large quantities of H_2 are consumed in the coal, minerals and petroleum industries during sulphur removal operations. The resulting toxic H_2S is often removed via Claus reaction and caustic or alkanolamine absorption. These routes permit only the recovery of elemental sulphur while H_2 is simply jettisoned as water. For a typical refinery, this translates to a loss of the order of a million dollars per annum in unrecoupable H_2. Raymont's cost analysis comparison [1] indeed showed that the overall economics of a plant with an H_2S decomposition-based technology is about 15% better than existing Claus process plants. Within the last two decades, five major options for H_2S splitting have emerged, namely:

1. direct non-oxidative thermal cracking [2,3];
2. solar-assisted decomposition [4];

*Corresponding author. Tel.: +61-2-9385-5268; fax: +61-2-9385-5966; e-mail: a.adesina@unsw.edu.au

0920-5861/99/$ – see front matter
PII: S0920-5861(98)00404-0

3. thermochemical open and closed loop processes [5];
4. electrolytic cleavage [6];
5. catalytic disproportionation [7–9].

The catalytic alternative has shown the greatest promise so far for commercial application. The catalysts considered have been mostly single transition metal sulphides with low surface areas. However, the use of bimetallic sulphides for HDS is well known [10] and Zdrazil [11] has discussed the significance of synergy in such systems. Catalytic activity is often stymied by poor surface areas. Rao et al. [12] have reported the superior performance of supported HDS catalysts prepared via precipitation from homogeneous solution (PFHS). These catalysts possess high surface areas compared to those obtained from direct sulphidation of the metal oxides. This method has therefore been used to prepare six γ-alumina supported bimetal sulphides. Ru was a constant co-pair element because of its position at the peak of the volcano plot for desulphurisation activity [13].

Apart from catalytic efficiency, reactor mode and operation also influence product yield. H_2S decomposition is a reversible endothermic reaction with low equilibrium conversion (ca. 14% at 1200 K). The continuous removal of one of the products from the reaction zone may therefore improve product yield. Although membrane reactor may be employed to achieve this goal, relatively few membranes can withstand the high temperature (873–1003 K) and corrosive nature of H_2S. However, in a fluidised bed, reaction takes place only in the solid-containing emulsion phase while the products are conveyed out of the reactor after migration into the non-reacting bubble-phase. Thus, a fluidised bed reactor (FBR) lends itself as a credible choice for H_2S decomposition for improved H_2 yield due to its relatively low molecular weight. Indeed, a recent investigation has shown that conversions in excess of that thermodynamically permissible are possible in a fluidised bed for certain types of variable–density systems with power-law kinetics [14]. In view of the foregoing considerations, the objectives of the present study were to:

(1) Prepare and evaluate a series of bimetallic sulphide catalysts.

(2) Carry out the kinetic analysis for the ''best'' catalyst in (1).

(3) Investigate the performance of a fluidised bed reactor with the chosen catalyst in order to improve H_2 yield or H_2S conversion.

2. Experimental

2.1. Apparatus and catalyst synthesis

The fluidised bed reactor is a 2 cm ID quartz tube (40 cm long) equipped with a 90 μm sintered quartz distributor. Quartz is resistant to high temperature and the corrosive H_2S. The reactor contained typically 0.2 g catalyst and 1.8 g of inert γ-alumina particles (110–420 μm). The whole reactor was placed in a temperature-controlled electrical furnace. Feed gases were of high purity H_2S and argon supplied by BOC Gases, Sydney. The flow rates were measured by Brooks mass flow controllers. The exit line from the reactor was electrically heated (773 K) to prevent sulphur condensation but passed through an acetone/ice mixture to remove solid sulphur before TCD–GC analysis (Shimadzu 8A model). The sulphur-free effluent was finally bubbled into a NaOH solution before atmospheric venting.

The metals paired with Ru, namely Ni, Cu, Mn, Fe, Zn and Mo were selected on the basis of their reported individual activity for H_2S decomposition [15]. With the exception of Mo obtained from ammonium heptamolybdate, all catalysts were prepared from aqueous nitrate solutions of the metals. A typical preparation entailed mixing calculated quantity of the appropriate aqueous nitrate solution with 1 g urea, 1 ml 0.75 M HNO_3 and 30 ml of thioacetamide solution. A weighed sample of commercial 0.5%Ru–γ-Al_2O_3 was then suspended in 100 ml of this solution and made up to the 250 ml level with distilled water in a conical flask. This mixture was placed in a heated water bath maintained at 367 K in a shaker (110 rpm) for 3 h. The precipitate was filtered, washed thoroughly with at least 3 l of distilled water and dried at 393 K for 14 h. The catalyst was further calcined in Ar at 1013 K for 3 h to ensure thermal stability during catalytic runs (<1013 K). The final specimen was then crushed and sieved to different particle size ranges.

2.2. Fluid dynamic characteristics of the fluidised bed reactor

The performance of a fluidised bed reactor is dependent upon a number of fluid and particle properties. The minimum fluidisation velocity, u_{mf}, may be calculated from

$$u_{mf} = \frac{d_p^2(\rho_s - \rho_g)g}{1650\mu_g}, \quad (1)$$

while the particle terminal velocity, u_t, may be obtained from

$$u_t = \frac{d_p^2(\rho_s - \rho_g)g}{18\mu_g} \quad (2)$$

for relatively small Reynolds number (Re<20) used in laboratory reactors. The minimum fluidisation velocity for the mean particle size of 270 μm at 943 K was calculated to be 2 cm s^{-1} (Eq. (1)). The terminal velocity for the smallest particle (d_p=90 μm) at the same temperature was estimated to be 20.2 cm s^{-1} (Eq. (2)). These values agreed with the experimentally determined values of 2.1 cm s^{-1} for u_{mf} and 24.3 cm s^{-1} for u_t. The fluidised bed has to operate between the limits of the minimum fluidisation and terminal velocity. Since gas velocities well in excess of $4u_{mf}$ may engender bubble coalescence and hence slugging, experiments were conducted with gas velocities, u, up to a maximum of 12 cm s^{-1} at the reaction temperature. The corresponding room temperature flow rate, F (ml min^{-1}), through the mass flow controllers was set by using

$$F = \frac{15u\pi d_p^2 T_0}{T}. \quad (3)$$

Fluidisation was always commenced using only pure Ar and once the reactor attained the desired reaction temperature, Ar flow was reduced and replenished with equivalent flow of H_2S to give the required feed gas composition. Rate data were taken only after the system reached steady-state as indicated by successive GC measurements.

3. Results and discussion

3.1. Catalyst evaluation

Table 1 displays the BET areas of the various catalysts. The decrease in surface area (13–21%) for the bimetallic catalysts compared to the monometallic 0.5%RuS_2/γ-Al_2O_3 sample is probably due to the higher total metal loading (1%) and hence pore blocking in the bimetallics. H_2S thermolysis did not commence until about 1013 K [3] and thus catalyst activity was measured in the range 883–1003 K and 160 kPa to avoid homogeneous gas phase contributions. All runs were carried out using a mean particle size of 270 μm and 5% H_2S/Ar feed at a flow rate of 5 cm s^{-1} (in the bubbling fluidisation regime). Prior analysis had shown that mass transfer effects did not influence reaction rates during fluidisation [16]. Similarly, blank runs with calcined γ-Al_2O_3 did not give measurable H_2S decomposition rates. Fig. 1 shows the activity variation with temperature for all samples. It is clear that the Ru–Mo sulphide catalyst is the most active. As may be seen from Table 2, it has the smallest activation energy (ca. 70 kJ mol^{-1}). With this relatively low partial pressure, the order with respect to H_2S should be the same for all catalysts. Column 3 in Table 2 displays the pre-exponential factors and it is obvious that a ''compensation effect'' exists since the trend in activation energy is opposite to that seen for the pre-exponential parameter. It would therefore seem that the better activity of the Ru–Mo catalyst

Table 1
Surface areas of the catalysts

Catalyst	BET surface area (m^2 g^{-1})
0.5MoS_2:0.5RuS_2:100γ-Al_2O_3	91
0.5MnS:0.5RuS_2:100γ-Al_2O_3	97
0.5CuS:0.5RuS_2:100γ-Al_2O_3	99
0.5NiS:0.5RuS_2:100γ-Al_2O_3	95.2
0.5FeS_2:0.5RuS_2:100γ-Al_2O_3	97.6
0.5ZnS:0.5RuS_2:100γ-Al_2O_3	101.4
0.5RuS_2:100γ-Al_2O_3	114.7

Table 2
Arrhenius parameters for the catalysts

Catalyst	Activation energy (kJ mol^{-1})	Pre-exponential factor (mol $gcat^{-1}$ s^{-1})
Ru–Mo	69.7	0.1881
Ru–Mn	103.53	3.216
Ru–Cu	110.03	4.957
Ru–Ni	100.04	1.563
Ru–Fe	89.23	0.401
Ru–Zn	104.72	1.954

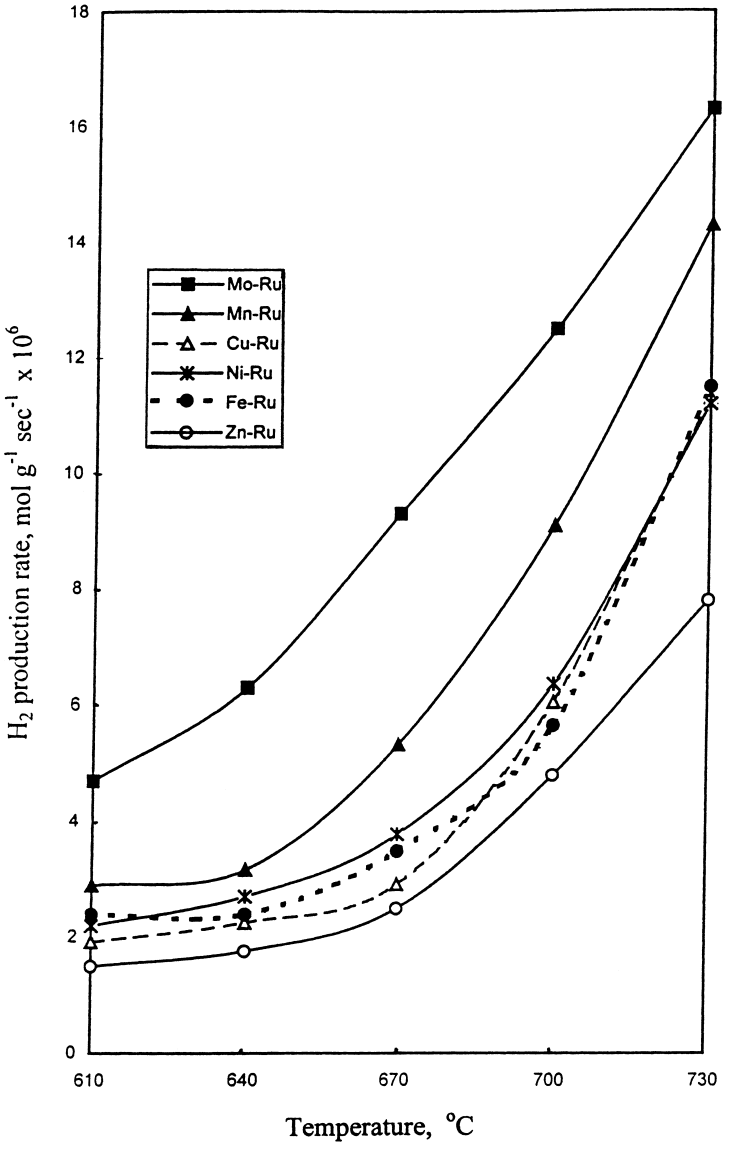

Fig. 1. Catalyst performance at various temperatures.

is due to the existence of intrinsically superior active sites for H_2S cleavage.

Chianelli and Pecoraro [13] observed that there is a relationship between the strength of the metal–sulphur bond at the surface of the catalyst and the HDS activity. Subsequently, Harris and Chianelli [17] obtained an excellent correlation between HDS activity and a parameter, *A*, which takes into account both the degree of the metal–sulphur covalency and the strength of the metal–sulphur bond. *A* is mathematically defined as the product of the number of d electrons in the highest occupied molecular orbital, *n*, and a previously specified variable, *B* [17]. The H_2S decomposition activity of the catalysts examined in this study was also reasonably correlated with this parameter as evident from Fig. 2.

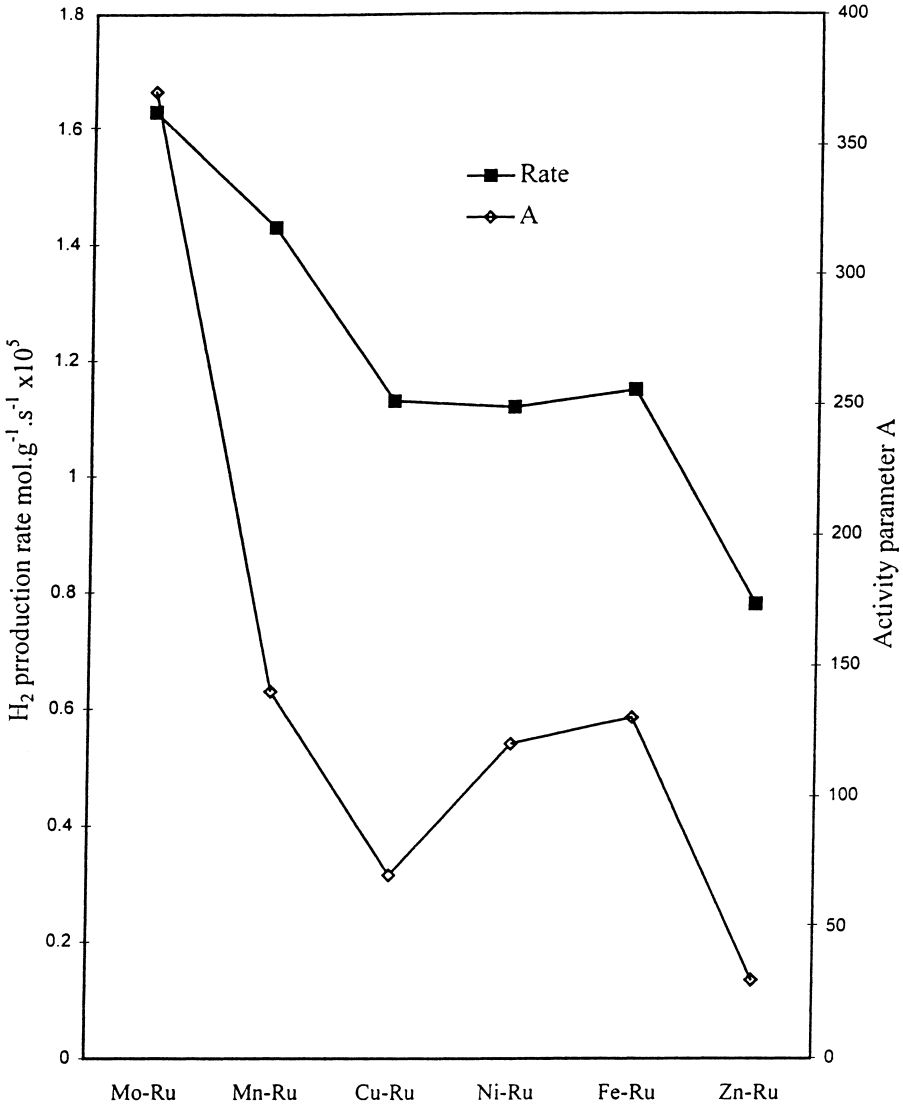

Fig. 2. Correlation between parameter A and catalyst activity.

3.2. Decomposition kinetics

The dissociation rates of H_2S over the Ru–Mo catalyst were further studied at conditions similar to those for the initial evaluation. As may be seen from Fig. 3, the rate increased monotonically with H_2S partial pressure at all temperatures. A fit of the data to the power-law expression

$$-r_{H_2S} = k_0 e^{-E/RT} P_{H_2S}^n \quad (4)$$

gave, n=0.952, E=66.85 kJ mol^{-1} and k_0=8.93×10^{-3} mol gcat^{-1} s^{-1} kPa$^{-0.952}$ with P_{H_2S} measured in kPa. Moffat and Adesina [18] have proposed a three-step mechanism for H_2S decomposition. The Langmuir–Hinshelwood (LH) steps may be written as

$$H_2S + X = H_2S - X, \quad (5a)$$

$$H_2S - X = H_2 + S - X, \quad (5b)$$

$$S - X = S + X, \quad (5c)$$

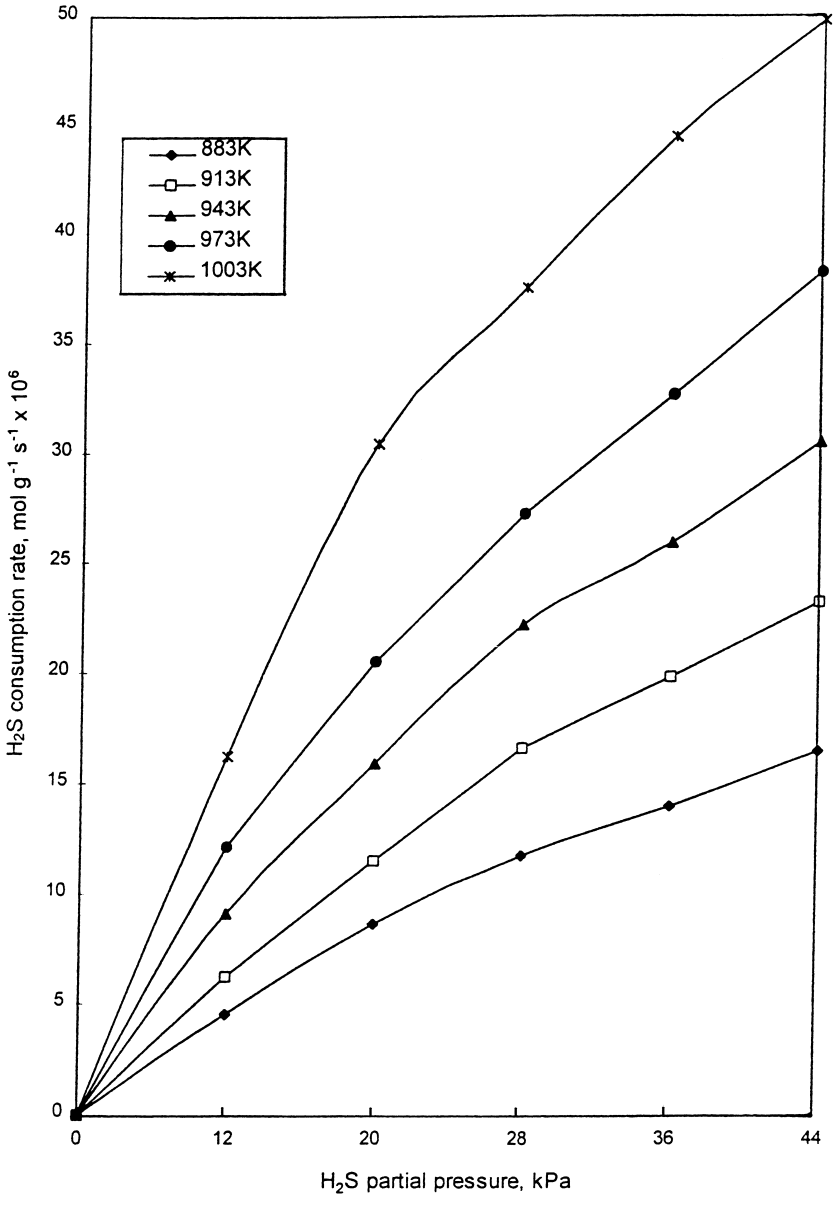

Fig. 3. Rate–composition–temperature behaviour of the Ru–Mo sulphide catalyst.

where X is the active site and the desorbed sulphur, S, probably exists as the thermodynamically more favourable diatomic, S_2 species [5]. LH models may be easily derived for three types of irreversible rate-limiting steps, namely:

Adsorption (Eq. (5a)):

$$-r_{H_2S} = \frac{k_a P_{H_2S}}{\left(1 + K_b K_c P_{H_2} P_{S_2}^{1/2} + K_c P_{S_2}^{1/2}\right)}. \quad (6)$$

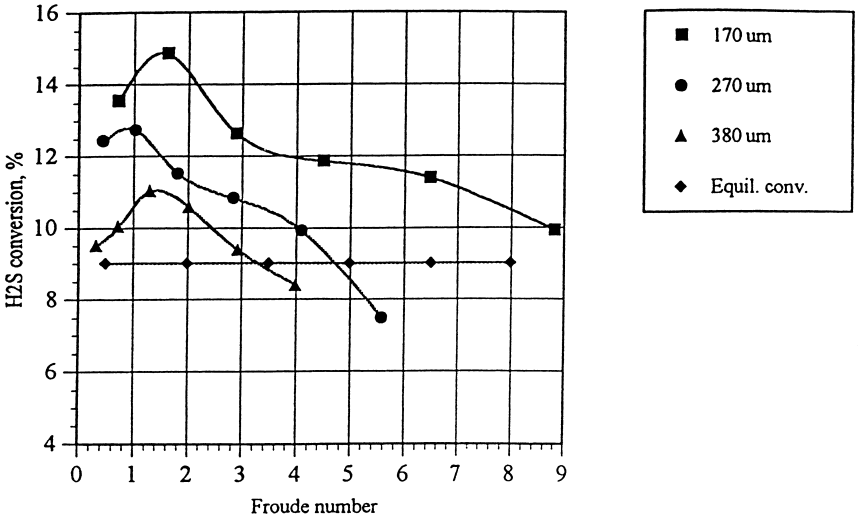

Fig. 4. Conversion–Froude number plot.

Surface reaction (Eq. (5b)):

$$-r_{H_2S} = \frac{k_b K_a P_{H_2S}}{\left(1 + K_a P_{H_2S} + K_c P_{S_2}^{1/2}\right)}. \quad (7)$$

Desorption (Eq. (5c)):

$$-r_{H_2S} = \frac{k_c K_a K_b P_{H_2S}}{\left(P_{H_2} + K_a K_b P_{H_2S} + K_a P_{H_2} P_{H_2S}\right)}, \quad (8)$$

where K_a, K_b and K_c are equilibrium adsorption constants for steps Eqs. (5a), (5b) and (5c), respectively, and k_a, k_b and k_c are the corresponding forward rate constants. Regression analysis of the data showed that only the adsorption model (cf. Eq. (6)) gave positive parameter estimates at all temperatures. It may therefore be reasonably assumed that the rate-controlling step over the Ru–Mo catalyst is the irreversible adsorption of H_2S. Due to the low conversions ($\leq$1%) employed, both P_{H_2} and P_{S_2} are very small compared to P_{H_2S}, and Eq. (6) is rewritten as

$$-r_{H_2S} = 5.713 \times 10^{-3} e^{-71057/RT} P_{H_2S}. \quad (9)$$

It may be observed that both the activation energy and the pre-exponential factor are close to the corresponding estimates from the empirical expression earlier obtained from Eq. (4).

3.3. Fluidisation studies

Fluidisation experiments were conducted with three particle sizes of mean diameters 170, 270 and 380 μm at 973 K using 7.5% H_2S/Ar. Gas flow rate was varied between 3.33 and 11.67 cm s^{-1}. Under these conditions, the particle sizes used could be described as type B Geldart classification. In particular, the operation spanned both smooth, bubble-free (Fr<1) and bubble–emulsion phase (Fr>1) fluidisation zones. It may be seen from Fig. 4 that maximum conversions were obtained for Froude number within 1–1.6. Since this corresponds to the transition from smooth to the two-phase bubble–emulsion fluidisation, it would seem that minimum bubbling conditions offered the best gas–solid contacting pattern. In the bubble-free or particulate fluidisation regime, the reaction mixture appears as a pseudo-homogeneous system and the H_2 produced remained essentially within this reaction zone. This would inhibit further H_2S conversion. However, in a bubbly fluidised bed with two phases, reaction takes place predominantly in the solid-containing emulsion phase followed by migration of reaction products into the catalyst-free bubble phase. The peaks observed at 1<Fr<1.6 suggest that these conditions permitted the greatest crossflow H_2 exchange between the two phases so that the reverse reaction between H_2 and sulphur is minimal in the

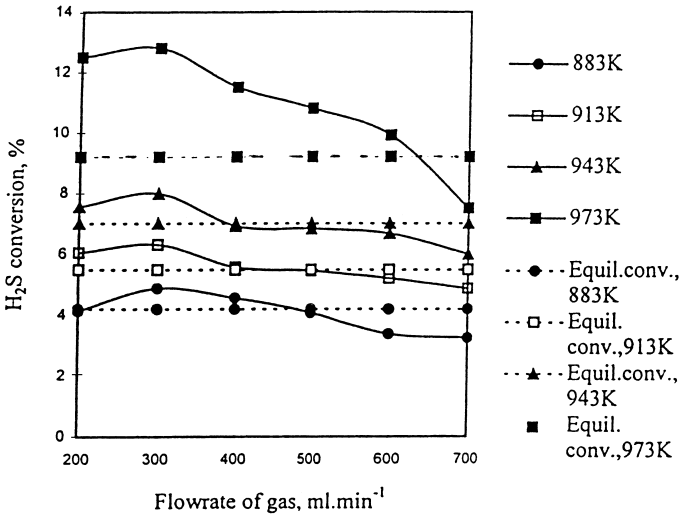

Fig. 5. Fluidised bed performance at different temperatures.

emulsion phase. The drop in conversion as *Fr* increased (>2) is an evidence of gas bypassing due to increased bubble size and bubble rise velocity. It is well known that slug formation (coalescence of small bubbles) at high gas velocities causes poor gas–solid contact. The excess gas velocity at which slugs would form in a bubbly fluidised bed is [19]

$$u - u_{\mathrm{mf}} \geq 0.07(gD_t)^{1/2}. \tag{10}$$

Interestingly, for the reactor and particle diameters employed here, Eq. (10) offers $Fr \geq 2$ in agreement with the experimental observations. Fig. 5 shows H_2S conversions in the fluidised bed reactor at four different temperatures using particles with mean diameter 270 μm. The predicted equilibrium conversions at these temperatures are shown as horizontal broken lines. The plot reveals that conversions higher than thermodynamic values were obtained for some flow rates. Fixed bed runs were conducted by passing the gas downwards for similar gas flow rates. It is evident from Fig. 6 that the fluidised bed operation was better than the fixed bed reactor. In particular, conversions in the fixed bed never exceeded thermodynamic limitation. From the foregoing, it would seem that the fluidised bed acted as a "membrane reactor" in order to overcome the equilibrium barrier. Consistent with our previous explanation, this scenario was possible because of a distinct inert bubble phase into which H_2 migrates upon production in the reacting emulsion

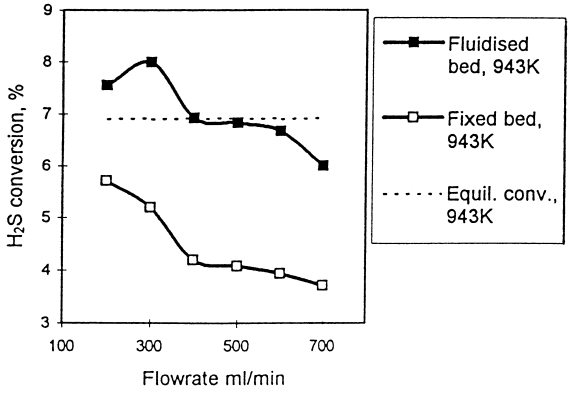

Fig. 6. Comparison between fixed and fluidised bed operations.

phase. Fluid dynamic property which dictates the crossflow exchange coefficients between these two phases is analogous to the permeability in a typical membrane reactor. However, it would seem that this advantage is confined to the relatively narrow window of operation with minimum bubbling conditions ($1 < Fr < 1.6$). In spite of this drawback, the technological constraints involved in the synthesis of high temperature resistant membranes vis-à-vis the established design base of the fluidised bed reactor justify its application for reaction systems where the membranous effect of the two-phase situation may be meritoriously tapped. Tafreshi [14] has reported that this advantage may be realised for a class of reversible

reactions involving low molecular weight ratios, e.g. methane reforming and ethyl benzene dehydrogenation.

4. Conclusions

Six bimetallic catalysts prepared via PFHS have been evaluated for H_2S decomposition. The Ru–Mo sulphide catalyst exhibited the best performance within the group. It has a relatively low activation energy of about 70 kJ mol^{-1} and intrinsically better active sites than the others. Kinetic studies over this catalyst showed that the irreversible H_2S adsorption was the most probable rate-controlling step. Fluidisation experiments covering both smooth bubble-free and the two-phase bubble–emulsion regimes indicated an optimum conversion as the Froude number increased from 0.2 to 9.0. This maximum was located between $1<Fr<1.6$ – an indication that the minimum bubbling conditions was favourable for H_2S conversion. Additionally, it was possible to exceed equilibrium conversion under these conditions. This was attributed to a ''membranous effect'' in the two-phase bubbling regime which permitted faster H_2 crossflow exchange rate than the reaction could generate and hence a shift to the right in the reversible decomposition. Furthermore, comparison with the fixed bed operation under the same conditions confirmed the superiority of the fluidised bed reactor.

5. Nomenclature

d_p	mean particle diameter (cm)
D_t	reactor diameter (cm)
F	room temperature gas flow rate (ml min^{-1})
Fr	Froude number (u^2/gd_p)
g	acceleration due to gravity
$-r_{H_2S}$	rate of H_2S decomposition (mol $gcat^{-1}$ s^{-1})
R	universal gas constant
Re	Reynolds number ($\rho_g u d_p/\mu_g$)
T	reaction temperature (K)
T_0	room temperature (K)
u_{mf}	minimum fluidisation velocity (cm s^{-1})

Symbol

ρ_g	gas density (g cm^{-3})
ρ_s	solid density (g cm^{-3})
μ_g	gas viscosity (P)

Acknowledgements

Duong Cao is grateful to AusAid for a postgraduate scholarship. Thanks are also due to the Australian Research Council for financial support and John Starling for technical assistance.

References

[1] M.E.D. Raymont, Hydrocarbon Process 54 (1975) 139.
[2] V. Kaloidas, N.G. Papayannakos, Chem. Eng. Sci. 44 (1989) 2493.
[3] A.A. Adesina, V. Meeyoo, G. Foulds, Int. J. Hydrogen Energy 20 (1995) 777.
[4] O.A. Salman, A. Bishara, A. Marafi, Energy 12 (1987) 1227.
[5] D. Berk, R. Heidemann, W. Svrcek, L. Behie, Can. J. Chem. Eng. 69 (1991) 994.
[6] H. Alqahthany, P.-H. Chiang, D. Eng, M. Stoukides, Catal. Lett. 13 (1992) 243.
[7] T. Chivers, J.B. Hyne, C. Lau, Int. J. Hydrogen Energy 15 (1987) 1.
[8] V. Meeyoo, A.A. Adesina, G. Foulds, Chem. Eng. Commun. 144 (1996) 1.
[9] V. Kaloidas, N.G. Papayannkos, Ind. Eng. Chem. Res. 30 (1991) 345.
[10] B. Delmon, Catal. Lett. 22 (1993) 1.
[11] M. Zdrazil, Catal. Today 3 (1988) 269.
[12] K.S. Rao, V. Prasad, K. Chary, P.K. Rao, Stud. Surf. Sci. Catal. 44 (1991) 661.
[13] R.R. Chianelli, T.A. Pecoraro, J. Catal. 67 (1981) 430.
[14] Z.M. Tafreshi, Ph.D. Thesis, University of New South Wales, 1997.
[15] V.A. Zhazhigalov, S.V. Gerei, M. Rubanik, Kinet. Katal. 4 (1975) 967.
[16] D. Cao, M.E. Thesis, University of New South Wales, 1997.
[17] S. Harris, R.R. Chianelli, J. Catal. 86 (1984) 400.
[18] S.C. Moffat, A.A. Adesina, Catal. Lett. 37 (1996) 167.
[19] D. Kunii, O. Levenspiel, Fluidization Engineering, Krueger, Huntington, NY.